

# Manufacturing influences on microstructure and fracture mechanical properties of polycrystalline tungsten

M. Conte\*, J. Aktaa

Karlsruhe Institute of Technology (KIT), Institute for Applied Materials (IAM-WBM), 76344 Eggenstein-Leopoldshafen, Germany



## ARTICLE INFO

### Key words:

Fracture toughness  
Polycrystalline tungsten  
Orientations dependency  
Crack path analysis

## ABSTRACT

Polycrystalline tungsten is a promising candidate for future fusion applications as plasma facing material due to its good thermophysical properties at high temperatures. Fracture mechanical properties of sintered and rolled, commercially available polycrystalline tungsten are characterized taking into account the strong anisotropy due to different grain shape and orientation with respect to the rolling direction. The fracture mechanics investigations are accompanied by fractographic analyses of two tungsten plate grades with varying cold working ratios of two different manufacturers (PLANSEE SE, Austria and A.L.M.T Corp., Japan). In this respect three point bending tests (3-PB) with sub sized fracture mechanical specimens in different orientations of the anisotropic microstructure are performed at three temperatures, ranging from 25 °C to 400 °C at a deflection rate of  $2 \mu\text{m s}^{-1}$ . In addition, crack initiation and crack growth mechanisms depending on texture and cold working ratio are investigated by means of scanning electron microscopy (SEM).

## 1. Introduction

In high-temperature applications like future fusion reactors, polycrystalline tungsten (W) shall be used as a plasma facing material due to its good thermophysical properties in a harsh environment at high temperatures and under irradiation influences [1]. Because of the high melting point, refractory metals like W are mainly produced via powder metallurgic process with sintering and subsequent cold and/or hot working steps. Several investigations of polycrystalline tungsten grades reveal a strong influence of anisotropic microstructure [2–4] deformation degree [5, 6] and grain size [7] to mechanical properties. Higher deformation degrees due to hot or cold rolling lead to an increase of strength and ductility of polycrystalline tungsten by reducing the grain size and increasing the aspect ratio [5]. Thus polycrystalline tungsten often exhibits a complex textured microstructure with elongated grains [1, 2]. Therefore the mechanical properties of polycrystalline tungsten are very sensitive to the deformation history during manufacturing. Due to a lack of information and details about the specific production routes of materials by both manufacturers this work focuses on fracture mechanical (FM) tests and fractographic as well as microstructural analysis.

## 2. Material and experimental procedure

In the frame of this work two different nominal pure tungsten grades of two manufacturers (PLANSEE SE (PS); > 99.97 wt.-% W) and A.L.M.T. Corp (ALMT) 99.9 wt.-% W) were investigated. Both plate materials, with thickness 5 mm (PS) and 12 mm (ALMT), respectively, were fabricated following a powder metallurgic process with sintering and subsequent cold and/or hot working steps [8,9].

Fracture mechanical characterization was conducted by quasi-static 3-PB tests at three temperatures (25 °C, 200 °C, and 400 °C). Due to the anisotropic microstructure and rolling direction of the plate materials two orientations (A, B) (cf. Fig. 1) were investigated. Miniaturized bend specimens with dimensions  $3 \times 4 \times 27 \text{ mm}^3$  and with 1 mm deep U type notches were used for fracture mechanical investigation. FM specimen production was carried out by cutting with electric discharge machining (EDM) and a subsequent surface preparation according to ASTM E399 [10] with several grinding steps along the rolling direction. Notch was introduced firstly by EDM with mean notch root radius of 0.18 mm and an additional notch refinement with razor blade polishing. The mean refined notch radius is roughly 20  $\mu\text{m}$  and the initial crack length 1000–1100  $\mu\text{m}$ . All notch dimensions (length, radius) were examined by optical microscope (Keyence VHX) and were averaged over both sides of the specimens.

Displacement-controlled tests were performed at a fixed transverse

\* Corresponding author.

E-mail address: [marco.conte@kit.edu](mailto:marco.conte@kit.edu) (M. Conte).

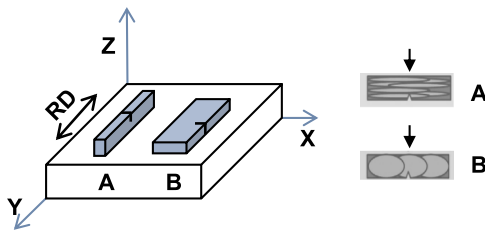


Fig. 1. Cutting scheme of fracture mechanical specimens and schematic microstructure related to the rolling direction (RD) and loading direction (arrow) of both plate materials.

speed of  $2 \mu\text{m s}^{-1}$  with a universal servo hydraulic testing machine equipped with a high-temperature vacuum furnace. During the experiments force, displacement and temperature were recorded. Fracture toughness  $K_Q$  was calculated according to ASTM E399 using the applied force at crack initiation and the notch length as crack length [10]. The conditional load  $F_Q$  was determined on the base of the 95% secant line in case of a semi-brittle and ductile material behavior. With pure brittle and linear elastic behavior  $F_Q$  is related to  $F_{max}$ .

Electron backscatter diffraction (EBSD) measurements as well as fracture surface analysis were carried out using a Zeiss EVO MA 10 scanning electron microscope (SEM). The EBSD patterns were acquired using a Bruker e-Flash detector and analyzed with the QUANTAX ESPRIT 1.9 software (parameters employed for EBSD measurements are: step size of  $0.15 \mu\text{m}$ , voltage of 20 kV and current of 3 nA).

Notch length as well as crack progress were investigated with a light microscope (Keyence VHX).

### 3. Result and discussion

#### 3.1. Fracture mechanical characterization

Selected load-displacement curves of both materials at all tested temperatures are shown in Fig. 2. In case of tests at elevated temperatures only the first segment of the load-displacement curves after initial load drop are depicted.

At room temperature both grades in A and B orientation have a linear elastic behavior with subsequent brittle fracture. Both materials exhibit no distinct difference of load values  $F_Q$  at crack initiation between the orientations. PS\_A and PS\_B, respectively, show higher  $F_Q$  values in comparison with ALMT\_A and ALMT\_B. After the initial load drop with a straight crack path ALMT\_A shows non-linear load displacement with a further load increase due to crack deflection into the rolling direction (cf. Fig. 6).

At 200 °C the critical load values at crack initiation of both grades are comparable in orientation A and B. ALMT\_A exhibit no pronounced load drop due to crack bridging near to the notch. PS\_A shows a higher load level at crack initiation, whereas in orientation B  $F_Q$  for both materials are comparable. In orientation B both exhibit a straight crack path with brittle fracture but partial plastic deformation and slight crack kinking and crack arresting which may lead to the further load increase after initial load drop.

At 400 °C PS\_B revealed higher crack initiation load and maximum load than ALMT\_B, whereas the elastic-plastic deformation behavior and failure mechanisms are comparable. Localized plastic deformation near crack tip and delamination perpendicular to roll axis with straight crack path lead to the non-linear deformation behavior of PS\_B and ALMT\_B. In Fig. 5c. it is apparent that delamination and weakening of grain boundaries perpendicular to roll axis and notch are the main failure mechanisms.

PS\_A exhibits crack initiation with transgranular brittle fracture and subsequent crack deflection along grain boundaries. Whereas ALMT\_A

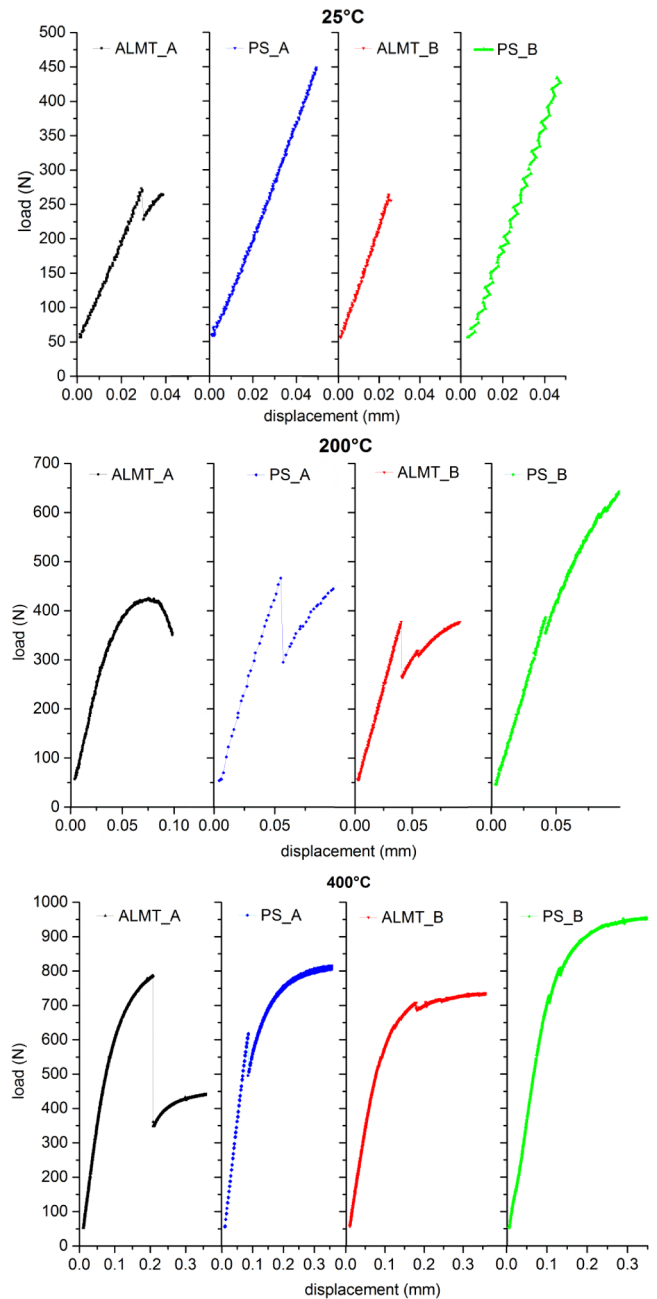


Fig. 2. Load-displacement curves of polycrystalline tungsten grades (ALMT and PS) in orientations A and B at 25 °C, 200 °C and 400 °C.

shows additional non-linear behavior before first load drop due to localized plastic deformation before crack initiation. In orientation A both load-displacement curves include several load drops which may indicate crack bridging and arresting.

Fig. 3 shows the determined fracture toughness  $K_Q$  over test temperature for both plate materials and orientations. With increasing temperature (RT up to 400 °C) fracture toughness of both grades and orientations rises. The RT values of both materials and orientations found to be valid according to ASTM E399. At elevated temperatures, however, with the onset of the non-linear deformation behavior, values of all orientations were found to be invalid.

At elevated temperatures, both materials exhibit non-linear deformation behavior with much higher load level compared to the RT tests. The non-linear behavior is probably due to microplasticity at the

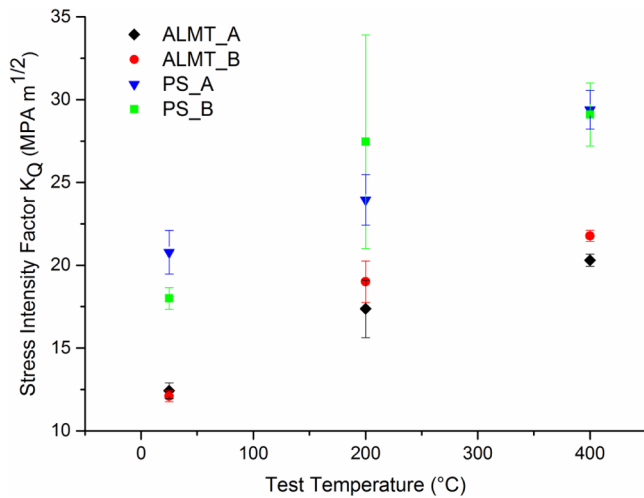


Fig. 3. Fracture toughness of polycrystalline tungsten grades in orientations A and B at 25 °C, 200 °C and 400 °C, calculated according to ASTM E399.

crack tip, blunting effects at the notch tip as well as delamination and crack deflection.

Over all temperatures plate, material of PLANSEE (PS\_A, PS\_B) exhibits higher fracture toughness values than the A.L.M.T. material (ALMT\_A, ALMT\_B). Fracture toughness of PS shows a more distinct orientation dependence compare to ALMT.

3.2. Microstructural analysis

EBSD measurements were carried out in two direction related to the rolling direction. Grain size measurement and aspect ratio have been evaluated with the line intersect method. The inverse figure poles (IPF) in Fig. 4 display an pronounced anisotropic microstructure with elongated grains in rolling direction for PS. ALMT material shows a microstructure with more equiaxed grains In top view along the Z axis both materials show rather uniform grain morphology with a bigger mean grain size in case of ALMT. However EBSD scans in X direction indicate a more pronounced grain elongation and higher aspect ratio for the PS specimens (ALMT 1:2.7; PS 1:5). All mean grain sizes of ALMT and PS in the top and side view are listed in Table 1.

Table 1

Mean grain size of ALMT and PS in the as-received state and evaluated with the line intersect method.

	ALMT		PS	
	X-Y	Z-Y	X-Y	Z-Y
Grain size [ $\mu\text{m}$ ]				
Parallel to RD	7.5	4.1	2.7	4.0
Perpendicular to RD	2.9	1.5	1.6	0.8

3.3. Fracture surface analysis

SEM fracture surface analysis was conducted for both materials tested at 25 °C, 200 °C and 400 °C and representative fracture surfaces as well as corresponding crack paths are depicted in Figs. 5 and 6.

At room temperature fracture surfaces of PS\_B and ALMT\_B are planar and indicate transgranular fracture with a crack path in X-Z plane and straight crack propagation in Z direction (cf. Fig. 5a). PS\_A also indicates a planar fracture surface within the X-Z plane and crack propagation in Z direction. PS\_A and ALMT\_A however show at first transgranular fracture and straight crack within X-Z and subsequent crack deflection and failure along grain boundaries in rolling direction (cf. Fig. 6a).

At 200 °C both grades in orientation A indicate crack deflection in rolling direction and less transgranular fracture compare to RT (cf. Fig. 6b). In orientation B brittle fracture with straight cracks paths within the X-Z plane occur. After crack initiation and load drop both materials exhibit crack tip blunting and branching with an increase of load level. At 400 °C distinct failure and decohesion of grains perpendicular to the rolling direction and tearing (cf. Fig. 5c) indicate delamination and local plastic deformation in case of ALMT\_B and PS\_B. PS\_B exhibits a finer or more pronounced tearing and delamination compare to ALMT\_B, due to the smaller grain size and higher aspect ratio. In comparison both materials in orientation A show crack kinking and deflection into the roll axis of the specimen, similar to the crack behavior at lower temperatures (cf. Figs. 5c and 6c).

4. Conclusion

In the frame of this work two polycrystalline tungsten plate materials with different grain structures have been investigated as a function

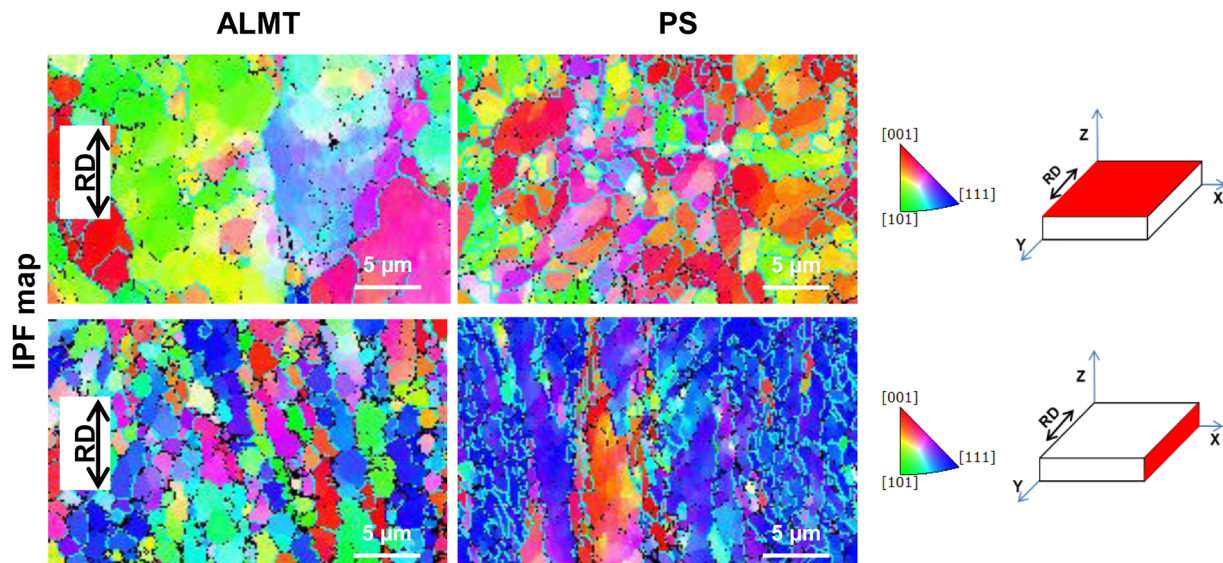


Fig. 4. Microstructure of ALMT and PS in the as-received state. IPF maps in top and side view. Viewing directions referring to the rolling direction are highlighted in red.

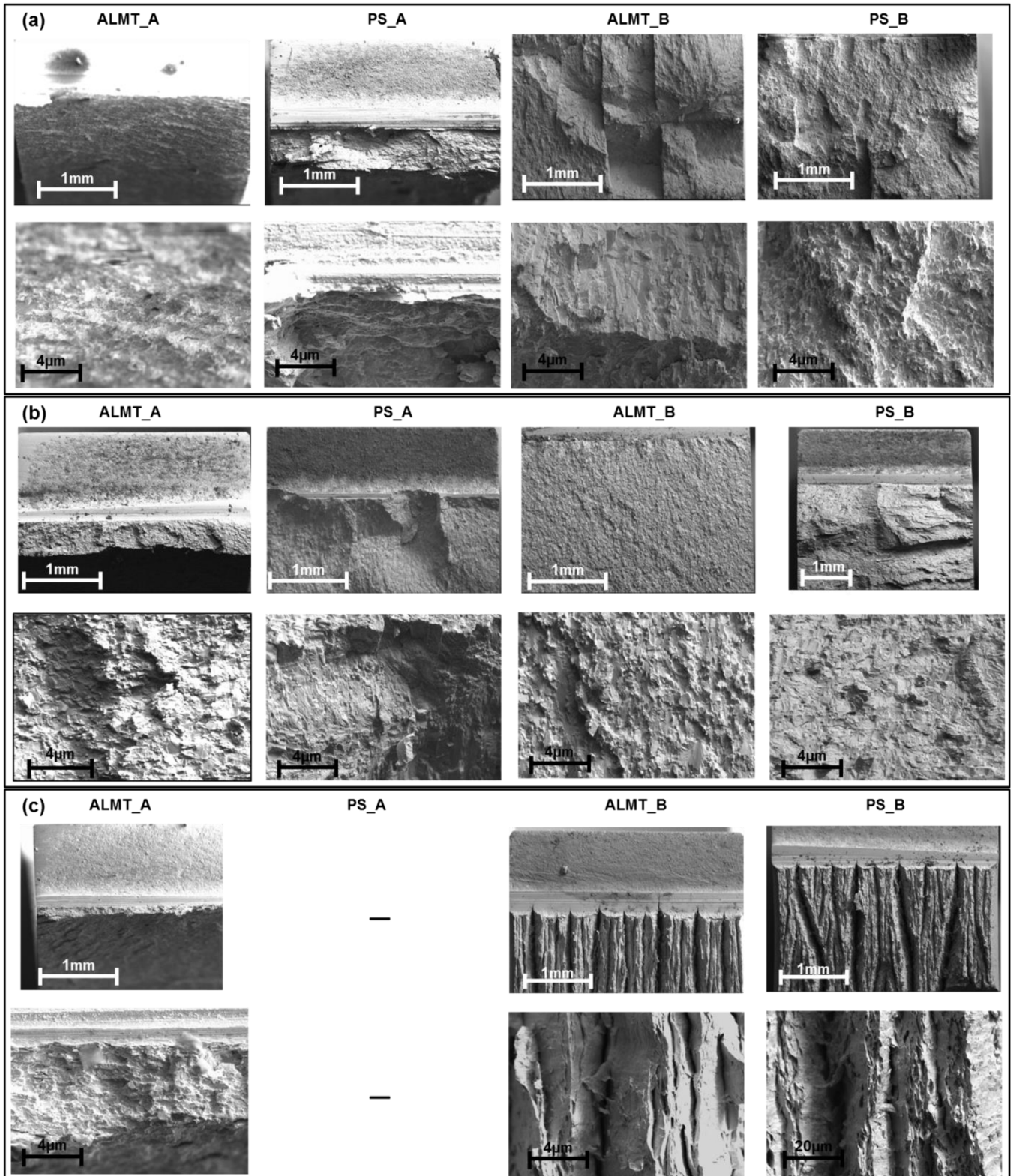


Fig. 5. Fracture surfaces of polycrystalline W (ALMT and PS) plates in different orientations (A and B) tested at 25 °C (a), 200 °C (b) and 400 °C (c) with 70x and 1000x magnification.

of temperature and crack orientation with respect to the rolling direction. The fracture mechanical characterization and microstructure and fractographic analysis revealed distinctive fracture behavior for both investigated orientations.

In orientation A both materials fail at RT next to the notch with

transgranular brittle fracture and subsequent crack kinking with intergranular failure within the grain boundaries along the rolling direction. Upon increasing temperature grain boundaries become weaker and with the orientation of the grains perpendicular to the loading orientation crack deflection are more pronounced. This leads to non-

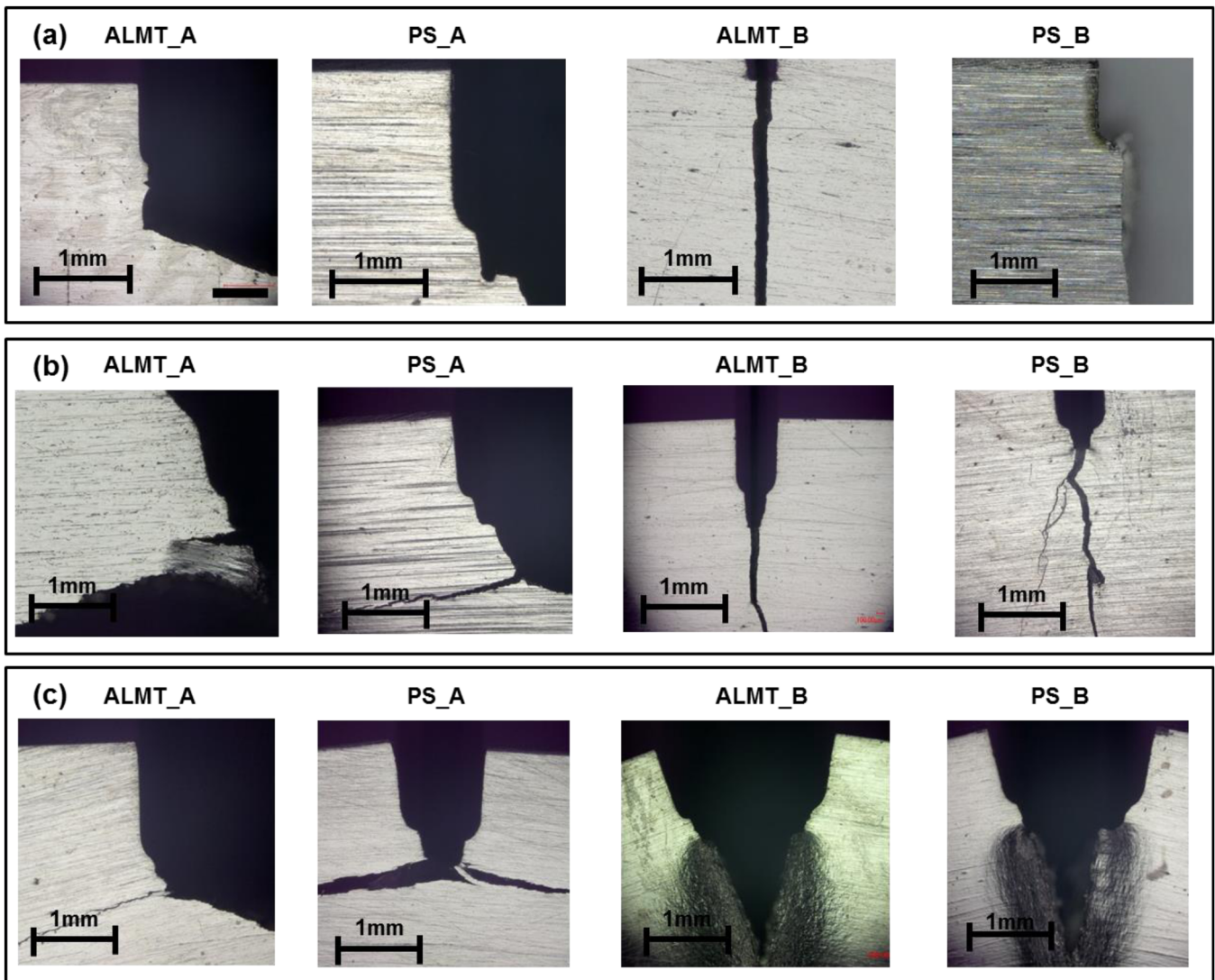


Fig. 6. Light microscope images of crack initiation and formation of polycrystalline W (ALMT and PS) plates in different orientations (A and B) tested at 25 °C (a), 200 °C (b) and 400 °C (c).

linear deformation behavior and increasing fracture toughness of both grades.

In orientation B both materials show transgranular cleavage fracture with a straight crack path perpendicular to the rolling direction at RT. At 200 °C additional crack deflection occurs which leads to an increase of the load after first load drop. At 400 °C local plastic deformation with reduction of cross section and tearing in the process zone and delamination occurs.

Beside general information, the specific production routes of both materials are unknown. Therefore the microstructure analysis can only give a hint about the pre-working conditions, heat treatment and deformation degree. Both materials reveal a similar material behavior in terms of failure mechanisms and crack orientation at all tested temperatures. Nevertheless the load levels at crack initiation and the addition subsequent plastic deformation in both orientations of PS are higher than of ALMT. The smaller mean grain size as well as the higher aspect ratio of PS suggests a higher degree of work hardening. Similar effects of grain size and dislocation density on cleavage stress and yield strength have been shown in [5] and [7].

## Acknowledgments

This work has been carried out within the framework of the EUROfusion Consortium and has received funding from the Euratom research and training programme 2014–2018 under grant agreement No 633053.

The views and opinions expressed herein do not necessarily reflect those of the European Commission.

## References

- [1] M. Rieth, D. Armstrong, B. Dafferner, S. Heger, A. Hoffmann, M.D. Hoffmann, U. Jäntschi, C. Kübel, E. Materna-Morris, J. Reiser, M. Rohde, T. Scherer, V. Widak, H. Zimmermann, Tungsten as a structural divertor material, *Adv. Sci. Technol.* 73 (2010) 11–21.
- [2] E. Gaganidze, D. Rupp, J. Aktaa, Fracture behaviour of polycrystalline tungsten, *J. Nucl. Mater.* 446 (1–3) (2014) 240–245.
- [3] D. Rupp, S.M. Weygand, Anisotropic fracture behaviour and brittle-to-ductile transition of polycrystalline tungsten, *Philos. Mag.* 90 (30) (2010) 4055–4069.
- [4] V. Krsjak, S.H. Wei, S. Antusch, Y. Dai, Mechanical properties of tungsten in the transition temperature range, *J. Nucl. Mater.* 450 (1–3) (2014) 81–87.

- [5] H. Noto, S. Taniguchi, H. Kurishita, S. Matsuo, T. Ukita, K. Tokunaga, A. Kimura, Effect of grain orientation and heat treatment on mechanical properties of pure W, *J. Nucl. Mater.* 455 (1–3) (2014) 475–479.
- [6] J. Reiser, J. Hoffmann, U. Jäntschi, M. Klimenkov, S. Bonk, C. Bonnekoh, M. Rieth, A. Hoffmann, T. Mrotzek, Ductilisation of tungsten (W): on the shift of the brittle-to-ductile transition (BDT) to lower temperatures through cold rolling, *Int. J. Refract. Met. Hard Mater.* 54 (2016) 351–369.
- [7] Q. Wei, L.J. Kecskes, Effect of low-temperature rolling on the tensile behavior of commercially pure tungsten, *Mater. Sci. Eng. A* 491 (1–2) (2008) 62–69.
- [8] Plansee SE, <https://www.plansee.com/shop/EN/category/Products/Tungsten%20and%20alloys/Sheets/Standard%20quality> (Accessed April 5, 2018).
- [9] A.L.M.T. Corp., <https://www.allied-material.co.jp/english/products/tungsten/processed/tanita/index.html> (Accessed April 5, 2018).
- [10] ASTM, Standard test method for linear-elastic plane-strain fracture toughness K<sub>IC</sub> of metallic materials, *ASTM Int* (2013) 1–33.